Research Journal of Chemical and Environmental Sciences
Res J. Chem. Environ. Sci. Vol 4 [4] August 2016: 50-57
Online ISSN 2321-1040
CODEN: RJCEA2 [USA]

Website: www.aelsindia.com/rjces.htm

RJCES

ORIGINAL ARTICLE

Preparation of ZnO, Its Characterization and Effectiveness in Waste Water Treatment

Md Jalil Miah[1,2*], Md. Nazmul Kayes[1,2], Md Obaidullah[1,2], Md Mofazzal Hossain[1]
[1]Department of Chemistry, University of Dhaka, Bangladesh
[2]Graduate School of Engineering, Utsunomiya University, Japan
*sjalil203@gmail.com

ABSTRACT
ZnO was prepared from $ZnSO_4.7H_2O$ and $(NH_4)_2CO_3$ by direct precipitation method followed by calcination of $ZnCO_3$ at 600^{0}C. Prepared ZnO was characterized by FTIR, LIBS and SEM techniques, respectively. ZnO was used as an adsorbent to remove the textile dye, Remazol Black-B (RBB), from aqueous solution. Adsorption of RBB on ZnO was carried out at three different temperatures 22^{o}C, 30^{o}C and 45^{o}C. Different kinetic models were used to interpret kinetics of adsorption. It was observed that the kinetics of adsorption follow pseudo-first-order model and adsorption complies with Langmuir isotherm. It was also found that with the increase of the temperature the amount of RBB adsorbed on ZnO decreased, which indicated the physical nature of adsorption. Furthermore, the experimental values of the thermodynamic parameter such as enthalpy of adsorption (H), Gibbs free energy of adsorption (G) also revealed the exothermic physisorption of RBB on ZnO.
Keywords: *Adsorption, Remazol Black-B, Kinetics, isotherm, Intraparticle Diffusion.*

Received 06.04.2016 Accepted 15.07.2016

INTRODUCTION

Thousand of dyes have been extensively utilized in various industries such as the textile, leather, paper, printing, food, solvent, rubber, plastic, cosmetics, petroleum, pesticide, wood-preserving chemical, paint, pigment and pharmaceutical industry, which generate a huge amount of dye effluent per year [1]. The effluents of textile dying and knitting industries contain a large amount of unfixed azo dyes, which come out into the environment without prior treatments. During the washing process, the exhausted reactive dyes are quite a large amount in their hydrolyzed and unfixed form [1,2]. The disposal of dye effluent into the environment without appropriate treatment can sternly affect aquatic life due to the reduction in light penetration and its toxicity. Much dye and colour effluent is toxic and has mutagenic, teratogenic and carcinogenic effects that influence the environment, ecosystems [3] and affect human life. Therefore, the removal of dyes from effluent is indispensable not only to defend human life but also from the environmental point of view to protect water resources.

A number of conventional treatment methods such as physical [4-7] (adsorption, coagulation, filtration etc) chemical [8-10] (oxidation, reduction) and biological [11,12] treatment have been applied to dispose of hazardous dyes from industrial effluent. Among all of these methods, the physical adsorption process at the solid–liquid interface is regarded as one of the most economic, efficient, and effective methods for decreasing the concentration of water body dyes in effluent or removing a wide range of organic and inorganic pollutants from wastewater [13,15]. Recently, intensive interest has been growing on the adsorption techniques for the abstraction of dyes from wastewater onto various adsorbent such as such as epiolite [16-18], kaolinite [19], Montmorillonite [20.21] Bentonite [22], bottom ash [23], peat [24], activated carbon [25,26], polymers [27], de-oiled soya [28], hen feathers [29], and rice straw [30].

In this context, ZnO was prepared, characterized, and used as an adsorbent to remove dyes from aqueous solution. The textile dye named Remazol Black-B ($C_{26}H_{21}N_5Na_4O_{19}S_6$, MW: 991.82g, λ_{max} = 594.50 nm, ε= 29412 L $mol^{-1}cm^{-1}$) in aqueous solution was used as model textile dyes.

MATERIALS AND METHODS

Remazol Black-B (RBB) (Dystar, Germany) was used without further purification. Commercial ZnO from (Fluka, Switzerland) was used as a fingerprint in LIBS for the characterization of prepared ZnO.

$ZnSO_4.7H_2O$ (≥ 30%, Merck, Germany), $(NH_4)_2CO_3$ (≥ 30%, Merck, Germany) and all others chemicals were purchased from Merck, Germany.

ZnO was prepared from $ZnSO_4.7H_2O$ and $(NH_4)_2CO_3$ by direct precipitation method followed by calcination of $ZnCO_3$. Stoichiometrically equimolar ratio of $ZnSO_4.7H_2O$ and $(NH_4)_2CO_3$ was dissolved separately in double distilled water. The beaker containing $ZnSO_4.7H_2O$ solution was kept in a water bath at 60°C. Then, the $(NH_4)_2CO_3$ solution was added slowly to the previous solution with constant stirring until complete precipitation of $ZnCO_3$. After vigorous stirring for 4 hours, the product was aged at ambient temperature for 96 hours. The resulting product was filtered and washed with deionized water repeatedly to remove SO_4^{2-} ions completely. The sample was dried in an oven and the dried product was then calcined at about 600 °C for 3 hours in a muffle furnace.

For LIBS analysis, both the prepared ZnO and commercial ZnO powders were turned into small balls using glue, separately. These balls were air-dried followed by drying in an oven at 110 °C, then irradiated with Nd:YAG laser which produces a plasma of all the elements present in the sample. The shape and surface morphology of the ZnO was investigated by field emission scanning electron microscope (JEOL, JSM-6490LA, Japan) under an acceleration voltage of 15 kV. For SEM analysis, the dried powder of ZnO was dispersed on a conducting carbon glued strip. The FT-IR spectra of the samples were recorded in the region of 4000 cm^{-1} – 400 cm^{-1} with 2 cm^{-1} resolution. Attenuated total reflection (ATR) was used to record the spectra of the ZnO.

All the aqueous solutions were prepared with double distilled water. A certain amount of ZnO was used to prepare ZnO suspension and soaked overnight to achieve the smoothness of the surface for the purpose of adsorption study. Batch adsorption experiments were conducted in order to evaluate the effects of contact time, an initial concentration of RBB, and temperatures. In each batch experiment, a definite concentration of RBB (5.0 -7.0 × 10^{-5} M) and a particular amount (0.05 g) of ZnO was taken in a 50 mL standard flask at room temperature and agitated for the fixed time intervals. After adsorption, the remaining dye in the solution was monitored by using a double beam UV–Vis spectrophotometer (UV-1610A, Shimadzu, Japan) at the maximum wavelength of RBB (λ_{max}=594.50 nm). Kinetic studies were carried out at three different initial dye concentrations, 5 × 10^{-5} M, 6 × 10^{-5} M and 7 × 10^{-5} M using 0.05 g of ZnO and isotherms studies were also conducted at three different temperatures of 22°C, 30°C, and 45°C. In all the adsorption experiments the pH of the solution was kept constant at 5.83.

RESULTS AND DISCUSSION

Characterization of Prepared ZnO

Laser-induced breakdown spectroscopy (LIBS) allows multi-elemental analysis of different materials including solid, liquid and gas. In order to characterize the prepared ZnO, LIBS experiment was recorded in the range between 380 - 500 nm for both the prepared and commercial ZnO. The LIBS spectra of the commercial ZnO (Fig 1a) shows peaks at 467.576 nm, 471.783 nm, and 480.604 nm, whereas, prepared ZnO (Fig 1b) shows peaks at 467.606 nm, 471.819 nm, and 480.618 nm. LIBS spectrum is capable of showing emission lines for almost all the elements present in the sample together with the aerial oxygen.

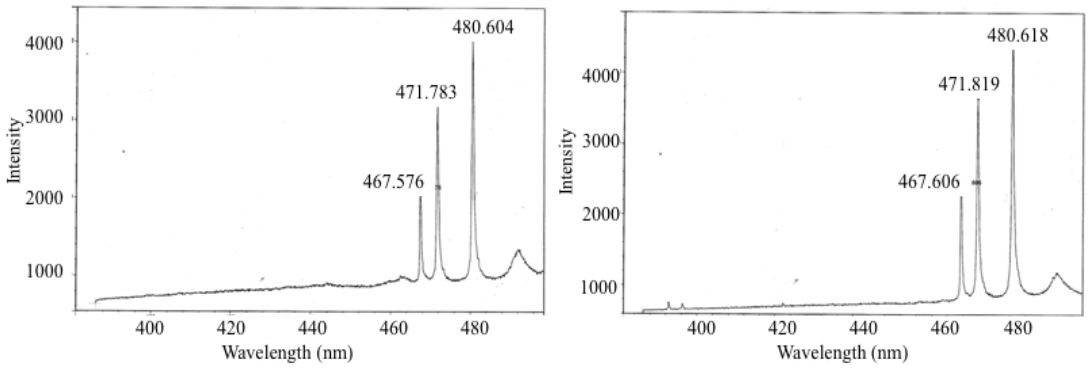

Figure 1: LIBS spectrum of (a) commercial and (b) prepared ZnO.

The spectrum of the commercial ZnO is used as a fingerprint for the prepared ZnO. The spectral data for both the ZnO are almost identical with each other suggesting the purity of the prepared ZnO. The ZnO (Fig 1b) also gave two small peaks at close to 400 nm, which may arise due to the presence of trace amount of impurity in the sample.

SEM image of ZnO (Fig 2) shows a non-crystalline and flaky shape of ZnO with porosity and the small size of particles (120 nm) can also be considered as nanoparticles.
FT-IR measurements were undertaken in order to further confirm the formation of ZnO. ATR-FTIR

Figure No. 2: SEM image of prepared ZnO.

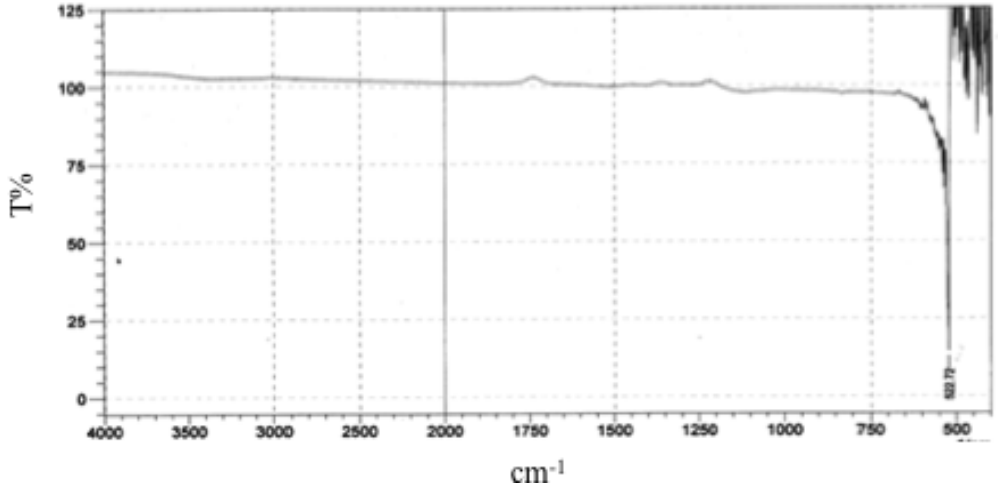

Figure 3: FTIR-ATR spectra of ZnO.

spectra of ZnO were recorded between 400 cm^{-1}- 4000 cm^{-1}. The peak at about 522 cm^{-1} in the FTIR spectrum (Fig 3) is attributed to the stretching vibration of Zn-O bond [31]. ZnO shows FTIR peak at 522 cm^{-1} along with additional peaks in the region of 1550 cm^{-1}- 1300 cm^{-1} [31]. The latter peaks were attributed to the presence of organic impurities. The absence of such peaks in prepared sample ensures the highly pure state of ZnO sample.

Effect of Initial Dye Concentration on Adsorption of RBB

It was observed that the dye uptake was increased from about 20 mg/g to 27 mg/g with the increase of dye concentration (Fig.4b), which might be ascribed to an increase in the driving force of the concentration gradient with the increase in the initial dye concentration [32,33]. Moreover, according to the chemical structure of the dye RBB (Fig. 4a), active sites and free hydroxyl ions were increased with the increase of the concentration of RBB. The effect of contact time on the uptake of RBB is also shown in the Fig 4b. The dye uptake increased with the increase in contact time.

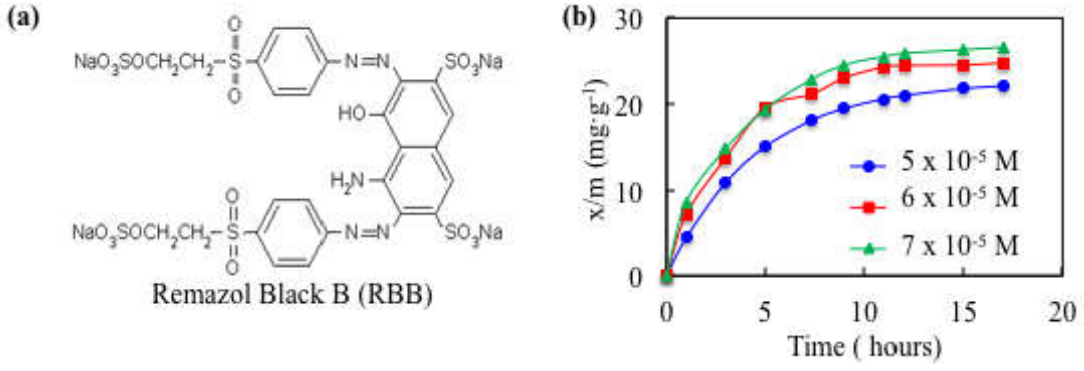

Figure 4: (a) Molecular structure of RBB, and (b) dye uptakes vs time for the absorption of RBB on ZnO.

The Maximum removal of RBB from aqueous solution was obtained after 13 hours. Initial adsorption was rapid due to the adsorption of dye onto the exterior surface, after that dye molecules enter into pores (interior surface), relatively slow process. The removal of RBB increased with the increase in concentration and remained constant after equilibrium time [34].

Effect of Temperatures

The adsorption studies were carried out at a set of temperatures in order to observe the effect of temperature on the adsorption and the results are shown in Fig 5. It was observed that with the increase of temperature the adsorption capacity decreased, which indicated the exothermic nature of adsorption. This decrease in adsorption with the increase of temperature is due to the decrease of surface activity of adsorbent [35].

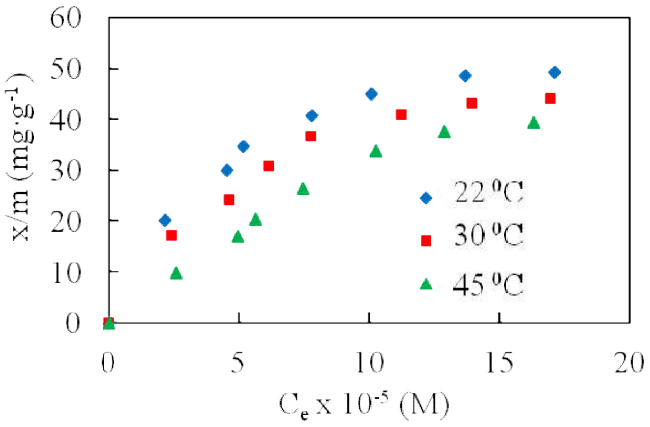

Figure 5: The adsorption isotherms of RBB on ZnO.

Kinetics of Adsorption of RBB on ZnO

Many kinetic models were developed in order to find intrinsic kinetic adsorption parameters. In this respect, two different kinetic models such as the pseudo-first and second order equation were tested to find out adsorption mechanism. Usually, kinetics of adsorption is described by the following Lagergren equations:

$\log (q_e - q_t) = \log q_e - k_1 t$.....(1) pseudo-first order model [36,37]

$t/q_t = 1/(k_2 q_e^2) + t/q_e$ .....(2) pseudo-second order model [38]

Where, q_t is the amount of dye adsorbed (mg/g) at various times t, q_e is the maximum adsorption capacity (mg/g) for both pseudo-first and second order adsorption, k_1 is the pseudo-first order rate constant for the adsorption (hrs^{-1}) and k_2 is the pseudo-second order rate constant (g mg^{-1} hrs^{-1}). According to the equation (1), plots of $\log (q_e - q_t)$ vs time give straight lines (Fig 6(a)). These straight lines are used to obtain the kinetic parameters for pseudo- first order equation. Similarly, according to the equation (2), plots of t/q_t against time also give straight lines (Fig 6(b)) which are used to obtain the kinetic parameter for pseudo-second-order equation. The rate constant (k_1, k_2), correlation coefficients (R_1^2, R_2^2), and initial adsorption rate, ($h = k_2 q_e^2$) of dyes under different conditions were calculated from these plots and are given in the following Table-1. The correlation coefficients of the first (R_1^2) and second-order kinetic model (R_2^2), suggests that the adsorption of RBB on ZnO follows the pseudo-first-order kinetic model.

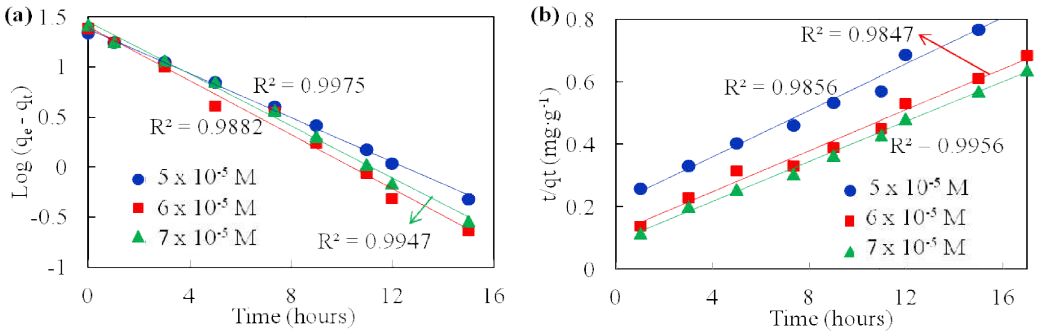

Figure 6: Applicability of (a) pseudo first order kinetic model and (b) second order kinetic model to adsorption of RBB on ZnO.

Table 1: Kinetic parameters of first and second-order models

C_o (g/L)	Pseudo-first order model		Pseudo-second order model		
	k_1 (mg/g.hrs)	R_1^2	$k_2 \times 10^5$ (g/gm.hrs)	$h = (k_2 q_e^2)$ (mg/g.hrs)	R_2^2
0.04	0.092	0.9975	7.81	0.0352	0.9856
0.05	0.112	0.9882	9.88	0.0323	0.9847
0.06	0.106	0.9947	8.36	0.0315	0.9956

Intraparticle Diffusion Model

The intraparticle diffusion model is given by the following equation

$q_t = k_p t^{1/2}$ ……(6)

Where, q_t is the amount adsorbed (mg/g) at time t and k_p is the intraparticle diffusion rate constant, (mg/g $min^{1/2}$). A plots q_t vs $t^{1/2}$ might provide a multilinearity [39,40] or would indicated the number of steps take place during the adsorption process such as (1) transport of adsorbate molecules from the bulk solution to the adsorbent external surface through the boundary layer diffusion; (2) diffusion of the adsorbate from the external surface into the pores of the adsorbent, and (3) adsorption of the adsorbate on the active sites on the internal surface of the pores [41]. Fig. 7 shows that the lines do not pass through the origin, which indicates that more than one process affects the adsorption but only one is rate limiting in any particular time range [42,43]. The slope of the linear portion reflected the rate of the adsorption. As shown in Table 2, the slope decreased from the first portion to the second portion. This implied that the intraparticle diffusion of RBB molecule into micropores was the rate-limiting step in the adsorption process [35].

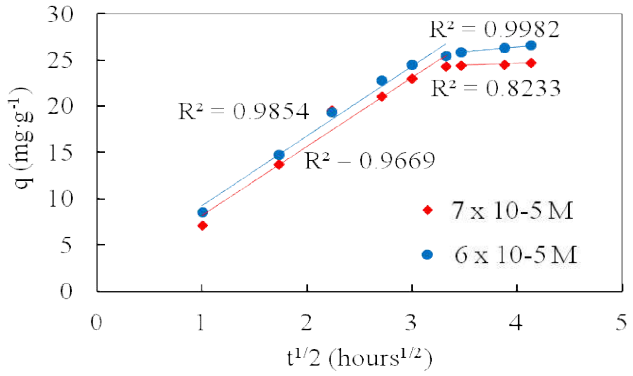

Figure 7: Plots of intraparticle diffusion model of adsorption of RBB on ZnO.

Table 2: Intraparticle diffusion parameters for adsorption of RBB on ZnO

Concentration	k_{p1} (mg/g $hrs^{1/2}$)	R_1^2	k_{p2} (mg/g $hrs^{1/2}$)	R_2^2
6×10^{-5} M	7.4533	0.9669	0.43323	0.8233
7×10^{-5} M	7.5412	0.9854	1.0506	0.9982

Adsorption Isotherms of RBB on ZnO at Different Temperatures

In order to investigate adsorption behavior of the RBB on ZnO, the experimental equilibrium adsorption data was analyzed using two adsorption isotherm models; the Freundlich [36] and the Langmuir [44], expressed by equations 3 and 4 respectively.

Freundlich isotherm: $q_t = K_F C^{1/n}$ …… (3)

Langmuir isotherm: $q_t = K_L.C.q_o / (1 + K_L.C)$…… (4)

Where, K_F parameter is related to the adsorption capacity and n is a measure of adsorption intensity. The Langmuir constant K_L, is related to the energy of adsorption and q_o is the maximum values of adsorption capacity (corresponding to complete monolayer coverage). Equation (3) and (4) can be written as

$\log q_t = \log K_F + (1/n) \log C_e$ …… (5)

$1/q_t = 1/q_o + (1/K_L.q_o).\ 1/C_e$ …… (6)

According to equation 5 and 6, the plots of Freundlich and Langmuir isotherms are as follows in Fig.8. Binding parameters for the adsorption of RBB on ZnO calculated from the slopes and intercepts of the straight lines are presented in Table 3, together with the correlation coefficients (R^2) as a goodness of fit criterion. The values of correlation coefficients (R^2) for the three models (Table 3) suggested that

experimental data were more suitable to the Langmuir models than to the Freundlich model. For all the experiments the values of n are greater than one which indicates good adsorption [45] of RBB on ZnO.

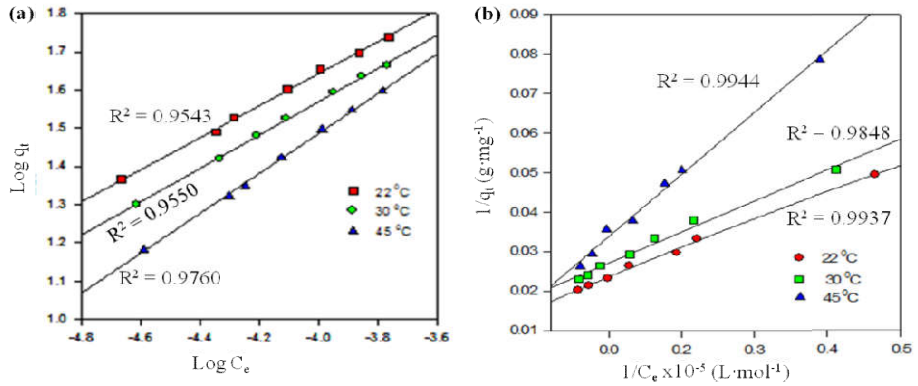

Figure 8: (a) Freundlich and (b) Langmuir isotherm of the adsorption of RBB on ZnO.

Table 3: Characteristic parameters of adsorption of RBB onto ZnO

Temperature (K)	Freundlich isotherm			Langmuir isotherm		
	K_F x 10^{-3} (mg/g).(L/M)$^{1/n}$	n	R_1^2	q_o (mg/g)	K_L x 10^{-6} (L/M)	R_2^2
295	3.827	1.908	0.9543	61.576	2.758	0.9937
303	2.088	2.286	0.9550	60.282	2.487	0.9848
308	1.827	2.908	0.9760	59.808	1.039	0.9944

Thermodynamic Study of Adsorption of RBB on ZnO

Using the values of constant, K_L, and the following equation, the thermodynamic parameters H (kJ/mol), G (kJ/mol) and S (kJ/mol) can be calculated for adsorption of RBB on ZnO.

$\ln K_L = -$ H / RT + constant .....(7)

G = - RT ln K_L ..... (8)

S = (H - G) / T ..... (9)

Where, R is the real gas constant and T is the absolute Temperature.

Table 4: The thermodynamic parameters of adsorption of RBB on ZnO

T (K)	G (kJ/mol)	H (J/mol)	S (J/mol.K)
295.00	-3.107	-0.951	7.31
303.00	-3.217		7.48
308.00	-3.492		8.25

The value of apparent enthalpy change (H) computed from the slope of linear dependence of $\ln K_L$ Vs 1/T (R^2 = 0.9568) is negative, which indicates the fact that the exothermic physical adsorption of RBB on ZnO and favored by the decrease in temperature. This relation would be explained by the increased solubility of RBB at higher temperatures. At the same time, the solubility of the adsorbent increases and hence the availability of adsorption sites decreases [46]. Again, the calculated value for enthalpy of adsorption is found lower than 100 kJ/moles, thus, it can be presumed that the adsorption is physical in nature [46]. Furthermore, the negative values of G confirm that the dye adsorption on ZnO is a spontaneous process. *G* up to -20 kJ/mol are associated with electrostatic interaction between adsorbent and the adsorbate molecules (physical adsorption), while *G* values more negative than -40 kJ/mol involve sharing or transfer of charge from the adsorbent surface to the adsorbate molecules in order to form a coordinate bond (chemical adsorption) [47]**.** Table 4 shows that the *G* values are <-20 kJ/mol, which indicates that physical adsorption is the predominant in the adsorption process [48]. The apparent entropy change (S) values are almost constant over the temperature range. The positive entropy characterizes an increased disorder of the system due to the loss of water, which surrounds the dye molecules before adsorption on the ZnO. It would be suggested that the driving force for adsorption is due to the effect of both enthalpy and entropy [49].

CONCLUSION

Flaky and porous ZnO was prepared, characterized by FTIR, SEM, LIBS experimental techniques and equilibrium kinetic as well as thermodynamic studies were executed for the adsorption of dye on ZnO. The characteristic parameters for each isotherm and related correlation coefficients suggest that adsorption follows Langmuir isotherm. The adsorption of RBB on ZnO satisfied the pseudo-first-order kinetic model more precisely. Intraparticle diffusion kinetic model reveals that RBB slowly transports via intraparticle diffusion into the pores and is retained in micropores. Thermodynamic parameters disclose the exothermic and physical nature of adsorption.

REFERENCES

1. Zollinger H (1991). Colour Chemistry: Synthesis, Properties and Application of Organic Dyes and Pigment, 2nd Ed., VHC Publishers, Weinheim.
2. Pagga U, Brown D (1986). The degradation of dyestuffs: Part II Behaviour of dyestuffs in aerobic biodegradation tests. Chemosphere 15: 479-491.
3. Zolinger H (1991). Color Chemistry: Synthesis, Properties and Applications of Organic Dyes and Pigments, VCH Publishers, New York.
4. Alaton IA, Balcioglu IA, Bahnemann DW (2002). Advanced oxidation of a reactive dyebath effluent: comparison of O_3, H_2O_2/UV-C and TiO_2/UV-A processes. Water Res. 36: 1143-1154.
5. Pollard SJT, Fowler GD, Sollars CJ, Perry R (1992). Low-cost adsorbents for waste and wastewater treatment: a review, Sci. Total Environ. 116: 31-52.
6. Vandevivere PC, Bianchi R, Verstaete W (1998). Treatment and reuse of wastewater from the textile wet-processing industry: Review of emerging technologies, J. Chem. Technol. Biotechnol. 72: 289-302.
7. Reife A, Freeman HS, A. (1996). Environmental Chemistry of Dyes and Pigments, Wiley, New York.
8. Allen SJ, McKay G (1996) Use of Adsorbents for the Removal of Pollutants from Wastewaters, CRC Press, Boca Raton, FL.
9. Alaton IA, Kornmuller A, Jekel MR (2002). Contribution of free radicals to ozonation of spent reactive dyebaths bearing aminofluorotriazine dyes. Color Technol. 118: 185.
10. Hasan MM, Hawkyard CJ (2002). Reuse of spent dyebath following decolorisation with ozone. Color Technol. 118: 104-111.
11. Hademal C, Boequillon F, Zahraa O (2001). Decolourization of textile industry wastewater by the photocatalytic degradation process. Dyes and Pigments 49: 117.
12. Guoging W, Henghi D, Liu C, Liu ZN (1990). A study of decolorizing dyes by utilization of purple nonsulphur photosynthetic bacteria. Water Treat. 5: 463.
13. Padmawathy, S., S. Sandhya and K. Swaminathan (2003). Aerobic decolorization of reactive azo dyes in presence of various cosubstrates. Chem. Biochem. Eng. Q. 17: 147.
14. Jain R, Mathur M, Sikarwar S, Mittal A (2007). Removal of the hazardous dye rhodamine B through photocatalytic and adsorption treatment. J. Environ. Manag. 85: 956–964.
15. Ozcan, AS, Tetik S, Ozcan A (2004). Adsorption of acid dyes from aqueous solutions onto sepiolit. Sep. Sci. Technol. 39: 301–320.
16. Rytwo G. Tropp D, Serban C (2002). Adsorption of diquat, paraquat and methyl green on sepiolite: experimental results and model calculations. Appl. Clay Sci. 20: 273–282.
17. Ozcan AS, Ozcan A (2005). Adsorption of acid red 57 from aqueous solutions onto surfactant-modified sepiolite. J. Hazard. Mater. 125: 252–259.
18. Armagan B, Ozdemir O, Turan M, Celik MS (2003). Adsorption of negatively charged azo dyes onto surfactant-modified sepiolite. J. Environ. Eng. 129: 709–715.
19. Harris RG, Wells JD, Johnson BB (2001). Selective adsorption of dyes and other organic molecules to kaolinite and oxide surfacesm. Colloids Surf. A: Physicochem. Eng. Aspects 180: 131–140.
20. Wang CC, Juang LC, Hsu TC, Lee CK, Lee JF, Huang FC (2004). Adsorption of basic dyes onto montmorillonite. J. Colloid Interface Sci. 273: 80–86.
21. Ogawa M, Kawai R, Kuroda K (1996). Adsorption and aggregation of a cationic cyanine dye on smectites. J. Phys. Chem. 100: 16218–16221.
22. Ozcan AS, Ozcan A (2004). Adsorption of acid dyes from aqueous solutions onto acid activated bentonite. J. Colloid Interface Sci. 276: 39–46.
23. Gupta VK, Mittal A, Krishnan L, Gajbe V (2004). Adsorption kinetics and column operations for the removal and recovery of malachite green from wastewater using bottom ash. Sep. Purif. Technol. 40: 87–96.
24. McKay G, Allen SJ (1983). Single resistance mass transfer models for the adsorption of dyes on peat. J. Sep. Process Technol. 4: 1–7.
25. Wang S, Li H (2007). Kinetic modelling and mechanism of dye adsorptions on unburned carbon. Dyes Pigm. 72: 308–314.
26. Tan IAW, Hameed BH. Ahmad AL (2007). Equilibrium and kinetic studies on basic dye adsorption by oil palm fibre activated carbon. Chem. Eng. J. 127: 111–119.
27. Lehocky M, Mracek A (2006). Improvement of dye adsorption on synthetic polyester fibers by low temperature plasma pre-treatment. Czech. J. Phys. 56: 1277–1282.
28. Mittal A, Krishnan L, Gupta VK (2005). Removal and recovery of malachite green from wastewater using an

agricultural waste material. de-oiled soya, Sep. Purif. Technol. 43: 125–133.
29. Mittal A (2006). Adsorption kinetics of removal of a toxic dye, malachite green, from wastewater by using hen feathers. J. Hazard. Mater. 133: 196–202.
30. Gong R, Zhong K, Hu Y, Chen J, Zhu G (2008). Thermochemical esterifying citric acid onto lignocellulose for enhancing methylene blue sorption capacity of rice straw. J. Environ. Manag. 88: 875–880.
31. Al-Hajry, Umar A, Hahn, Kim, (2009). Growth, properties and dye-sensitized solar cells-applications of ZnO nanorods grown by low-temperature solution process. Superlattice and Microst. 45: 529–534.
32. Hameed BH, Mahmoud DK, Ahmad AL (2008). Sorption of basic dye from aqueous solution by pamelo (Citrus grandis) peel in batch system. Colloids Surf. A: Physicochem. Eng. Aspacts 316: 78–84.
33. Ashtoukhy ESZE (2009). Loofa egyptiaca as a novel adsorbent for removal of direct blue dye from aqueous solution. J. Environ. Manag 90: 2755–2761. Culp SJ, Beland FA (1996). Malachite green: a toxicological review. J. Am. Coll. Toxicol. 15: 219–238.
34. Meikap BC, Mohanty K, Naidu JT, Biswas MN (2006). Removal of crystal violet from wastewater by activated carbons prepared from rice husk. Ind. Eng. Chem. Res. 45: 5165–5171.
35. Kumar PS, Gayathri R (2009). Dsorption of Pb^{2+} ions from aqueous solutions onto bael tree leaf powder: isotherms, kinetics and thermodynamics study. J. Eng. Sci. Technol. 4: 381 – 399
36. Namasivayam C, Kanchana N (1992). Waste banana pith as adsorbent for colour removal from wastewaters. Chemosphere, 25: 1691-1696.
37. Wong YC, Szeto YS, Cheung WH, Mckay G (2004). Pseudo-first-order kinetic studies of the sorption of acid dyes onto chitosan. J. Appl. Polum. Sci. 92: 1633-1645.
38. Ho YS, Mckay G (1998). A two-stage batch sorption optimized design for dye removal to minimize contact time. Trans IchemE, 76: 313-318
39. Annadurai G, Juang RS, Lee DJ (2002). Use of cellulose based wastes for adsorption of dyes from aqueous solutions. J. Hazard. Mater. 92: 263-274.
40. Wu FC, Tseng RL, Juang RS (2001). Adsorption of dyes and phenols from water on the activated carbon prepared from corn cob wastes. Environ. Technol, 22: 205-213.
41. Cheung W H, Szeto YS, McKay G (2007). Intraparticle diffusion processes during acid dye adsorption onto chitosan. Biores. Technol. 98: 2897-2904.
42. Li Q, Yue QY, Su Y, Gao BY, Fu L (2007). Cationic polyelectrolyte/ bentonite prepared by ultrasonic technique and its use as adsorbent for reactive blue K-GL dye. J. Hazard. Mater. 147: 370-380.
43. Zhong QQ, Yue QY, Li Q, Xu X, Gao BY (2011). Preparation, characterization of modified wheat residue and its utilization for the anionic dye removal. Desalination 267: 193-200
44. McKay G, Blair HS, Hindon A (1989). Equilibrium studies for the sorption of metal ions onto chitosan. Indian J. Chem. 28: 356-360.
45. Zor S (2004). Investigation of the adsorption of anionic surfactants at different pH values by means of active carbon and the kinetics of adsorption. J. Serb Chem Soc. 69: 25-32.
46. Tran HN, You S, Chao H (2016). Thermodynamic parameters of cadmium adsorption onto orange pell calculated from various methods: A comparison study. J, Enviorn, Chem. Eng. 4: 2671-2682.
47. Horsfall M, Spiff AI, Abia AA (2004). Studies on the influence of mercaptoacetic acid (MAA) modification of cassava (Manihot sculenta cranz) waste biomass on the adsorption of Cu^{2+} and Cd^{2+} from aqueous solution. Bull. Korean Chem. Soc. 25: 969-976.
48. Abdel Ghani NT, Elchaghaby GA (2007). Influence of operating conditions on the removal of Cu, Zn, Cd and Pb ion from wastewater by adsorption. Int. J. Environ. Sci. Tech. 4: 451-456.
49. Suteu D, Bilba D, (2005). Equilibrium and kinetic study of reactive dye brilliant red HE-3B adsorption by activated charcoal. Acta Chim. Slov. 52: 73-79.

CITE THIS ARTICLE

Md Jalil Miah, Md. Nazmul Kayes, Md Obaidullah, Md Mofazzal Hossain. Preparation of ZnO, Its Characterization and Effectiveness in Waste Water Treatment.Res. J. Chem. Env. Sci. Vol 4 [4] August 2016. 50-57